Catalysis Today 164 (2011) 436–442

Contents lists available at ScienceDirect

Catalysis Today

journal homepage: www.elsevier.com/locate/cattod

Ethanol catalytic condensation over Mg–Al mixed oxides derived from hydrotalcites

Marta León, Eva Díaz*, Salvador Ordóñez

Department of Chemical Engineering and Environmental Technology, University of Oviedo, Julián Clavería s/n, 33006 Oviedo, Spain

ARTICLE INFO

Article history:
Available online 2 November 2010

Keywords:
Bioethanol upgrading
Base catalysis
Aldol condensation
Guerbet reaction
C4 alcohols
C4 olefins

ABSTRACT

Different Mg–Al mixed oxides derived from hydrotalcites were prepared and tested for ethanol catalytic condensation. Different procedures for preparing the catalysts lead to different distributions of acid and basic sites, and therefore to different reactivity. The studied catalysts are active for both dehydration reaction yielding ethylene (because of the presence of acid sites) and hydrogenation reactions yielding acetaldehyde (catalysed by medium-strength basic sites). Acetaldehyde is the key reactant for condensation reaction, yielding 2-butenal as primary condensation product. This reaction is catalysed by the strongest basic sites. This unsaturated aldehyde undergoes successive hydrogen transfer reactions and/or dehydrations yielding different C4 chemicals: 2-buten-1-ol, butanal, 1-butanol, 1,3-butadiene and 1-butene.

Although the total conversion obtained with the different materials is rather similar, important differences are observed in the obtained selectivities. Those materials with higher concentration and strength of the basic sites are those more selective for C4 fractions, whereas the presence of acid sites promotes ethanol dehydration, decreasing the efficiency for condensation reactions.

1. Introduction

Catalytic transformation of ethanol into higher added value products has been investigated for more than three decades [1,2], this interest being recently increased because of the renewable character of bioethanol (obtained from different biomass materials with similar qualities as petrochemical ethanol) as raw material [3]. Base-catalysed ethanol condensation leads to larger molecules, such as 1-butanol or 1,3-butadiene. The replacement of liquid bases by solid-base catalysts would facilitate the separation and recovery of the catalysts from the reaction products and would strongly decrease corrosion phenomena and environmental constraints [4–6]. In addition to the environmental advantages, the use of solid catalysts opens the possibility of preparing solid base materials with a different nature of active sites (Bronsted, Lewis or chiral sites), with a range of basic strengths, or even acid–base bifunctional catalysts [7].

An important industrial process that is used to increase the carbon number of alcohols is the Guerbet reaction. In this reaction, a primary or secondary alcohol reacts with itself or another alcohol to produce a higher alcohol [8]. It is generally accepted that the Guerbet reaction consists of the following three steps: dehydrogenation of alcohols to the corresponding aldehydes, aldol condensation of the resulting aldehydes, and hydrogenation of the unsaturated condensation products to give the higher alcohols [9]. In particular, 1-butanol has been reported to be obtained from ethanol over a variety of solid catalyst, such as alkali earth metal oxides and modified MgO [8], hydroxyapatites with different Ca/P molar ratios [3,10], or Mg–Al mixed oxides [11]. 1-Butanol is an important chemical feedstock widely used as solvent and as a crucial building block for acrylic acid and acrylic esters [12–14], as well as having applications as an additive to gasoline [15].

Ethanol also serves as a raw material for the synthesis of 1,3-butadiene (raw material for the manufacture of SBR elastomers) through the Levedev process, where ethanol is dehydrogenated, dehydrated and dimerized in one step over a MgO/SiO_2 catalyst [16]. This is a traditional process still commercially used in certain parts of the world, although 1,3-butadiene is primarily produced as a by-product in the steam cracking of hydrocarbon streams to produce ethylene. Nowadays, Levedev synthesis could gain interest as a competitive process from bioethanol feedstock, which should be accompanied by further research concerning new catalysts. Surprisingly, the reaction of ethanol to generate 1,3-butadiene has been hardly reported in the literature. Thus, Tsuchida et al. described the synthesis of 1,3-butadiene from ethanol over hydroxyapatites, depending on the distribution of acid and basic sites on the catalyst surface [3,10].

* Corresponding author at: University of Oviedo, Department of Chemical Engineering and Environmental Technology, C/Julián Clavería s/n, Facultad de Química, 33006 Oviedo, Asturias, Spain. Tel.: +34 985 102 914; fax: +34 985 103 434.
E-mail address: diazfeva@uniovi.es (E. Díaz).

0920-5861/$ – see front matter © 2010 Elsevier B.V. All rights reserved.
doi:10.1016/j.cattod.2010.10.003

Hydrotalcite-derived Mg–Al mixed oxides have received increasing attention in the search for environmentally benign catalysts due to their high surface area, acid–base properties, and structural stability [17], as well as because they can be easily and cheaply synthesized [9]. These materials contain the metal components highly dispersed and in intimate contact, thereby promoting complex bifunctional reactions, which require the catalyst functions to exist in mutual contact at molecular scale [18]. Indeed, Mg–Al mixed oxides have been reported to catalyze a variety of organic transformations such as aldol condensation, Claisen–Schmidt condensation, Knoevenagel condensation, olefin isomerization, alkylation of diketones, and epoxidation of activated olefins with hydrogen peroxide [19]. Acid–base properties in Mg–Al mixed oxides, which are generally known to be important for catalytic activity and selectivity, strongly depend on their chemical composition and preparation procedures [20,21]. For a mixed oxide with a given chemical composition, the number of active sites can be controlled by modifying the specific surface area of the solid, whereas the strength of the centres can be adjusted by modifying the number of defects in the framework. At this point, it has been reported [22] that ultrasonication during the coprecipitation step enhances not only the surface area but also the number of defects in the mixed oxides, leading to sites of higher basicity.

In the present work, hydrotalcite-derived Mg–Al mixed oxides with Mg/Al molar ratio of 3 were synthesized by coprecipitation under conditions of low and high supersaturation. It is generally accepted that low supersaturation leads to precipitates with higher crystallinity than those obtained under high supersaturation [23]. Furthermore, the influence of ultrasound irradiation of the mixture was taken into account by preparing a new series of materials following both precipitations at low and high supersaturation methods under sonication. The effect of the different preparation methods on the surface acid–base properties of the samples was correlated with their catalytic performance in the reaction of conversion of ethanol, in terms of activity and selectivity to the different products.

2. Experimental procedure

2.1. Catalysts preparation

Mg–Al hydrotalcites with Mg/Al molar ratio of 3 were synthesized by coprecipitation at low and high supersaturation conditions, respectively [24]. For co-precipitation at low supersaturation (constant pH), 1 M solutions of $Mg(NO_3)_2{\cdot}6H_2O$ (Fluka, >99%) and $Al(NO_3)_3{\cdot}9H_2O$ (Panreac, 98%) were mixed in 3/1 molar ratio. A volume of 150 mL of this solution was added drop-wise to 100 mL of K_2CO_3 (Panreac, 99%) 0.2 M under vigorous stirring at 333 K. The pH was kept at 10 by adding appropriate quantities of 1.6 M NaOH (Prolabo, 98%) solution. For coprecipitation at high supersaturation (variable pH), 150 mL of the Mg and Al solution in 3/1 ratio were added to 200 mL of a base solution containing 1.6 M NaOH and 0.1 M Na_2CO_3 (Probus, 98%) under stirring. In both cases, the mixture was aged at 353 K for 24 h before a centrifugation step. Two additional series of materials were prepared combining both precipitations, at low and high supersaturation, with sonication. This procedure was carried out at room temperature and the gels obtained were not aged.

The precipitate was separated in each case by high-speed centrifugation, washed in deionized water several times until pH 7 in order to remove the alkali metals and nitrate ions, and dried in oven at 373 K for 24 h. Mixed oxides were finally derived from the resulting hydrotalcites by heat treatment at 723 K in air flow. The temperature was raised at 5 K/min up to 723 K, where maintained for 8 h.

The samples were labelled as "HT1" or "HT2" depending on whether they have been synthesized by low or high supersaturation method, respectively, followed by "US" in the case of samples prepared under sonication. For the calcined samples, "c" was placed in front.

2.2. Catalysts characterization

Chemical analysis of the samples was determined in a HP 7500c inductively coupled plasma mass spectrometer (ICP-MS). The crystalline structure of the hydrotalcites and the derived mixed oxides was studied by XRD using a Philips X'Pert Pro powder diffractometer equipped with a CuKα radiation source (0.154 nm) and operating in a 2θ range of 5–85° at a scanning rate of 0.02°/s. The X-ray tube voltage and current were set at 45 kV and 40 mA, respectively. Textural properties of the materials, surface area (S_{BET}), average pore diameter (D_P) and total pore volume (V_P), were measured by N_2 adsorption–desorption isotherms at 77 K on a Micromeritics ASAP 2000.

Determination of the density of basic sites on the surface of the catalysts, along with their strength and nature was carried out by thermogravimetric adsorption of CO_2 and Fourier transform infrared spectroscopy (FT-IR) of chemisorbed CO_2. Thermogravimetric adsorption of CO_2 (Praxair, >99.99%) on mixed oxides was measured using a thermogravimetry-differential scanning calorimetry (TG-DSC) instrument (Setaram, Sensys). Samples were pretreated in situ at 723 K in pure N_2 flowing at 20 mL/min before measuring the CO_2 adsorption at 0.1 MPa and 323 K. A constant flow of 20 mL/min was maintained during the CO_2 sorption experiments for 10 h, followed by desorption under N_2 flow for 2 h and, subsequently, under thermal conditions (723 K, at 5 K/min). The procedures used for the characterization of the basicity of these materials have been optimized in a previous work [24].

The surface acid properties of the catalysts were studied by temperature programmed desorption of preadsorbed NH_3 and, additionally, by the catalytic test of isopropanol decomposition. TPD-NH_3 experiments were carried out in a Micromeritics TPD/TPR 2900 apparatus. Samples (100 mg) were pretreated overnight in He at 723 K prior to saturation with NH_3 (5% in He) at 323 K for 0.3 h. Weakly adsorbed NH_3 was removed by flushing with He at the same temperature for 1 h. The temperature was then increased at a linear rate of 5 K/min up to 723 K while NH_3 evolution was monitored by mass spectrometry (Pfeiffer Vacuum-300). Catalytic decomposition of isopropanol was carried out in order to gain further understanding about the balance between basic and acid sites [10], and was performed in a U-shaped quartz reactor (4 mm i.d.) housed in an electric furnace controlled by PID. The sample (100 mg) was placed on a plug of quartz wool and a thermocouple was placed inside the catalyst bed. Feed (30 mL STP/min) consisted of 2.8 vol.% of isopropanol (Prolabo, 99.7%) gas diluted with nitrogen. Prior to the reaction, the samples were pretreated at 723 K for 1 h in nitrogen flow. Outgoing gases were analysed on-line by mass spectrometry.

2.3. Reaction studies

Ethanol conversion experiments were performed between 473 and 723 K in the same experimental setup described above for the isopropanol reaction. The catalysts (100 mg, with a particle size of 100–250 μm) were pretreated at 723 K for 1 h in helium flow before the reaction. Ethanol (Panreac, 99.5%) was vaporized in helium and the resulting stream, with 5.5 vol.% of ethanol, was fed to the reactor at 30 mL STP/min. (W/F_{A0} = 24.7 g h/mol; WHSV = 0.215 h^{-1}). Outgoing gases were analysed on-line through a mass spectrometer, previously calibrated for the reaction products response. Additionally, products identification was confirmed

Table 1
Chemical and morphological properties of the mixed oxides used as condensation catalysts in this work.

Sample	Mg/Al (mol)	L200 (nm)	S_{BET} (m^2/g)	D_p (nm)	V_p (cm^3/g)
cHT1	2.9	5.1	137	24.9	1.007
cHT1US	3.0	4.1	142	19.3	0.816
cHT2	2.9	4.4	190	15.8	0.757
cHT2US	3.0	4.4	174	9.3	0.410

by gas chromatography–mass spectrometry (GC–MS, Shimadzu QP-2010).

In order to discard the presence of both internal and external mass transfer effects, experiments performed with the most active catalyst (cHT2US) were replicated with other particle sizes (350–500 μm) and working with the one half of the total flow rate and catalyst weight (and the same concentration of ethanol). Results obtained in these two experiments were similar to the obtained in the parent experiment, suggesting the absence of both external and internal mass transfer effects.

3. Results and discussion

3.1. Catalysts characterization

Results concerning the chemical and morphological characterization of the catalyst are summarized in Table 1, further details being described in our previous work [24]. Chemical analysis confirmed the correct incorporation of Mg and Al cations from the precursor solutions, since molar ratios Mg/Al = 3 were determined for all the samples. X-ray diffraction patterns of raw materials showed the typical diffractograms of hydrotalcite-like materials (JCPDS 14-191) [24]. Regarding the mixed oxides, XRD patterns revealed that the layered structure was completely collapsed after heat treatment. Only weak, broad peaks reflections at ∼37°, 43° and 62° were observed, which corresponds to diffraction by planes (1 1 1), (2 0 0) and (2 2 0) of the periclase (MgO, JCPDS 45-946). No aluminium phases were discerned in the diffractograms, suggesting that aluminium compounds should be well dispersed or forming an amorphous phase [25]. The crystallite size of the mixed oxides was calculated from the plane (2 0 0) using the Debye–Scherrer equation [26] and their values are included in Table 1. Sonication treatment generally leads to slightly lower crystillinities, caused by acoustic cavitation effects, which induces particle fragmentation [22]. This effect is more marked in the mixed oxides prepared by low supersaturation method, however no differences were found between catalysts synthesized at high supersaturation conditions. Nitrogen adsorption–desorption isotherms determined at 77 K correspond to a type IV isotherm (mesoporous solids) according to the IUPAC classification. From the values exposed in Table 1, precipitation at high supersaturation conditions gave rise to mixed oxides displaying larger specific surface areas, although smaller pore sizes and pore volumes.

The combined physisorption and chemisorption isotherms of CO_2 at 323 K were determined by TG-DSC. After desorption under N_2 flow at the same temperature, the weakly bonded physisorbed CO_2 was removed, remaining merely the chemisorbed fraction, which can be correlated with the density of basic sites on the surface of the catalysts. From the first column in Table 2 (amount of chemisorbed CO_2 expressed in mmol per gram of sample), it can be concluded that ultrasound treatment during the coprecipitation step markedly enhanced the surface basicity on the catalysts. Furthermore, high supersaturation method also benefited the generation of basic sites, compared to low supersaturation method.

To further characterize the basic sites, infrared spectroscopic studies of the surface of the mixed oxides after CO_2 adsorption and desorption at temperatures up to 673 K were determined in our previous work [24]. Experimental results showed that bridging bidentate carbonates were formed on the weakest basic sites, since they disappear above 323 K. Bicarbonates and chelating bidentate disappeared above 373 and 473 K, respectively, whereas a fraction of unidentate carbonates remained even after evacuation at 673 K. The values of the assigned infrared bands corresponding to the highest vibration modes of the spectra obtained after CO_2 adsorption at room temperature, as well as the area of the decomposed peaks corresponding to each species, which is proportional to the concentration of each type of basic site present in the samples, are summarized in Table 2. According to these results, ultrasound treatment not only increased the total number of basic sites, but also the proportion of the stronger ones, which is consistent with the remarks reported by Climent et al., 2004 [22]. Regarding the precipitation method, high supersaturation conditions increased the density of strong base sites.

Main results of the integration of TPD-NH_3 profiles are reported in the last column of Table 2. Similar considerations can be drawn for all the catalyst regarding their surface acid properties, except for cHT2. This sample presented the largest amount of adsorbed ammonia, along with the highest temperature for the maximum, which can be correlated with a greater density and average strength of the surface acid sites, respectively.

Besides direct measurements of acidity adsorbing gaseous probe molecules as NH_3, catalytic test reactions, such as decomposition of isopropanol, have been used for indirect characterization of the catalysts acidity in reaction conditions [27,28]. Depending on the acid–base properties of the catalyst, isopropanol can undergo three types of competitive reactions, namely: dehydrogenation, which gives rise to acetone and hydrogen; intramolecular dehydration, which yields propene and water; and intermolecular dehydration to isopropyl ether [29]. It has been reported that dehydrogenation to acetone involves intermediate-strength base sites [30]. Nevertheless, propene formation can proceed via different mechanisms. On strongly acid solids, isopropanol dehydrates through an E_1 mechanism in which only the acidic sites take part, whereas on amphoteric oxides the reaction occurs via a concerted

Table 2
Surface acid–base properties of the mixed oxides studied in this work.

	Chem. CO_2 (mmol/g)	Unidentate carbonates	Chelating bidentate carbonates	Bicarbonates	Bridged bidentate carbonates	TPD-NH_3
cHT1	0.67	*1575*, *1505* (23)	*1650* (55)			**85** [4.1×10^{-11}]
cHT1US	0.79	*1590*, *1530* (44)	*1645* (13)	*1685* (19)	*1730* (7)	**87** [4.5×10^{-11}]
cHT2	0.68	*1590*, *1525* (27)	*1655* (19)	*1690* (14)	*1740* (5)	**98** [5.6×10^{-11}]
cHT2US	0.90	*1590*, *1500* (74)	*1650* (14)	*1690*(36)	*1755* (3)	**87** [4.8×10^{-11}]

In italics (cm^{-1}): infrared bands after CO_2 adsorption at room temperature. In brackets (a.u.): area of the decomposed FT-IR peaks. In bold (°C): temperature of the maximum of the TPD-NH_3 desorption peak. In square brackets (a.u.): area under the TPD-NH_3 peaks.

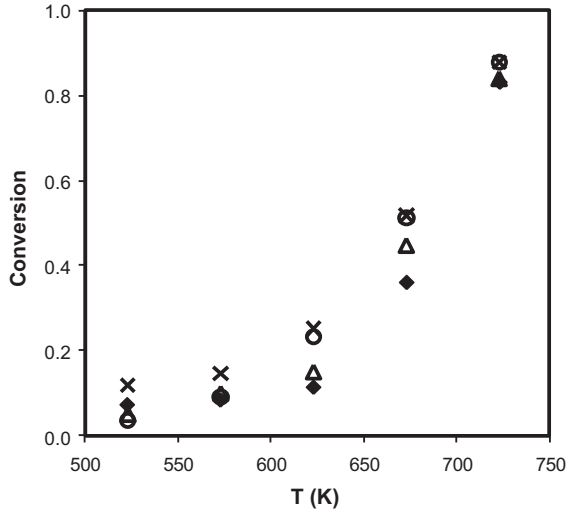

Fig. 1. Evolution of conversion with temperature over the tested catalysts: cHT1 (♦), cHT1US (○), cHT2 (△) and cHT2US (×).

E_2 mechanism implying acid–base pairs. Additionally, dehydration can take place on strongly basic catalyst containing acid–base pairs of imbalanced strength through an E_{1cB} mechanism. Finally, the E_2 mechanism also leads to isopropyl ether formation [10]. Reactions carried out in the present work yielded acetone as the main product for the four catalysts tested. Isopropyl ether was not detected in any case, whilst propene was only appreciable with two of the catalysts: cHT2, reaching a maximum selectivity of 35% at 633 K, and cHT1US, 10.5% at the same temperature. Sample cHT2 showed the greater acid character according to TPD-NH_3 experiments, which, together with the fact that no outstanding base properties were evidenced from FT-IR measurements, suggests that dehydration on this catalyst could occur mainly through an E_2 mechanism. On the other hand, the pathway responsible for the formation of propene on sample cHT1US should be different, since no significant differences in its acidic properties were found compared to the rest of the samples. In conclusion, this reaction is not appropriate for the quantification of surface acid/base properties because of the concomitance of the reaction pathways to the propene formation.

3.2. Catalytic reaction

Fig. 1 shows the typical pattern of the reaction, whereas selectivities to the main reaction products are summarized in Figs. 2–5. It is observed that conversion trends are very similar, being the differences lower at low conversions, at which the cHT2US material provides the highest conversions, which is in a good agreement with its highest concentration of basic sites. As temperature increases, there is a competition between acid- and basic-sites catalyzed reactions leading to lower differences between tested catalysts in terms of global conversion.

Carbon balances, considering the amount of ethanol used as reactant, and the concentration of ethanol and all the identified reaction products, present closures higher than 90% in all the reported experiments. The presence of lower amounts of heavier condensation products cannot be discarded, in agreement with the findings of other authors for this reaction [3,10]. In order to rule out the presence of fast deactivation caused by these heavy condensation products, separate deactivation experiments were performed with all the catalysts at 675 K for 8 h. In all the cases, conversion and selectivity trends remain almost unaltered (conversion decreases lower than 6% in the worst case). Considering that the total time of the reported experiments was about 10 h, and working at lower

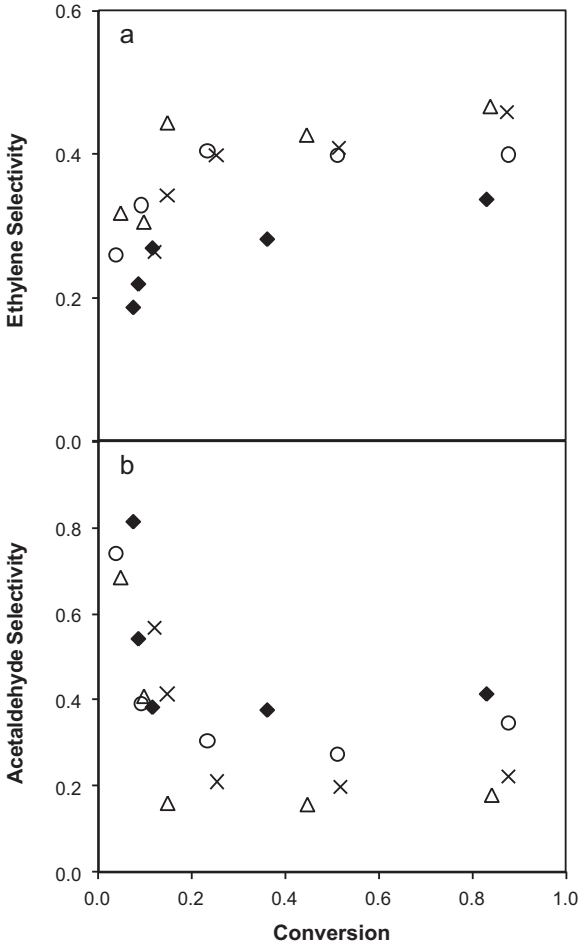

Fig. 2. Selectivity-conversion curves for the two primary products, ethylene (a) and acetaldehyde (b) over the tested catalysts: cHT1 (♦), cHT1US (○), cHT2 (△) and cHT2US (×).

temperatures in most of the cases, it can be concluded that catalyst deactivation is not affecting the catalyst performance in the reported experiments.

From the obtained results, the reaction mechanism depicted in Scheme 1 can be proposed. In general terms, two primary products were obtained from ethanol: ethylene and acetaldehyde. Ethylene is mainly formed by direct dehydration of the ethanol over the acid sites, although mechanisms involving strong basic sites can be not ruled out, as will be discussed later. Ethylene formed during this reaction does not react, whereas acetaldehyde follows successive condensations, as indicated by the continuous decrease of the acetaldehyde selectivity as ethanol conversion increases. Although there are also authors [8] claiming that it is possible the direct condensation of two ethanol molecules (involving proton abstraction from the β-carbon, and the nucleophilic attack to the second ethanol molecule) yielding a molecule of 1-butanol, we consider that this mechanism is not relevant in our case by two reasons: the observed acetaldehyde selectivity profile (suggesting that acetaldehyde participate in subsequent reactions), and the presence of significant amounts of butadiene (which can be not formed from 1-butanol). As primary products, the selectivity for these compounds is markedly higher than the corresponding to the other products. It should be noted that acetaldehyde selectivity decreases with temperature because it undergoes further condensation reactions.

The primary condensation product detected is 2-butenal. According to the accepted base-catalyzed aldol condensation mechanism, the primary product will be the 3-hydroxybutanal,

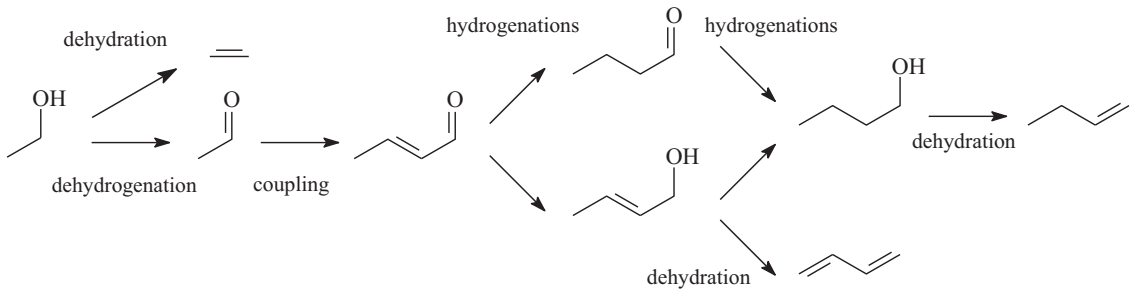

Scheme 1. Overall mechanism for ethanol conversion over Mg–Al mixed oxides.

but this compound is easily dehydrated to form the 2-butenal over acid-strong basic pairs. This compound follows two alternative reaction pathways based on hydrogenation reactions, yielding either butanal (hydrogenation of the double bond) or 2-buten-1-ol (hydrogenation of the carbonyl group). Hydrogenation of the unsaturated compounds could occur involving surface hydrogen atoms (proton- and hydride-like) resulting from ethanol dehydrogenation [10], although reduction of the C=O bond could also proceed via a Meerwein–Ponndorf–Verley (MPV) mechanism, through a cyclic six-membered intermediate between adjacent adsorbed aldehyde and ethanol, which results in hydride transfer (α-hydrogen) without participation of surface H fragments [31]. According to this, it is expected that this reaction could be connected with the transformation of ethanol into acetaldehyde. Concerning to the hydrogenation of the double bond of the 2-butenal yielding butanal, as well as the hydrogenation of the 2-buten-1-ol yielding 1-butanol, these reactions are well established in presence of hydrogen and metal catalysts, but can be unexpected in absence of these factors. However, Tsuchida et al. [10] and Di Cosimo et al. [11] reported the hydrogenation of saturated aldehydes, and α,β-unsaturated aldehydes by reaction with hydrogen species coming from the dissociative adsorption of alcohols yielding acetaldehydic species. Similar mechanism can be applied to the formation of 1-butanol by hydrogenation of butanal.

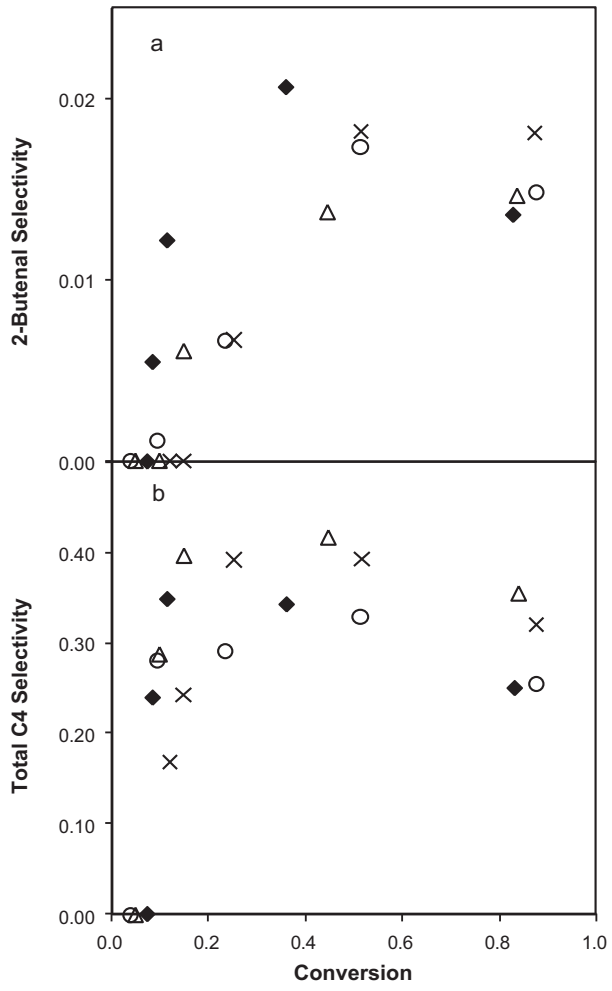

Fig. 3. Selectivity-conversion curves for the primary condensation product, 2-butenal, (a) and overall C4 products (b) over the tested catalysts: cHT1 (♦), cHT1US (○), cHT2 (△) and cHT2US (×).

Concerning to the C_4 olefins, it is expected that both observed compounds (1-butene and 1,3-butadiene) are formed by dehydration of 1-butanol and 2-buten-1-ol, respectively, with a similar mechanism that the proposed for the formation of ethylene from ethanol. In good agreement with this conclusion, selectivity vs. conversion shows for both alcohols (more markedly for 1-butanol) the typical behaviour of a secondary product undertaking further reactions, whereas the olefins show the pattern of a secondary product not suffering further reactions.

Activity and selectivity trends observed for the different catalysts can be explained in terms of the concentration and strength of their acid and basic centres previously described. Therefore, ethanol dehydration to ethylene seemed to occur preferably in the catalysts synthesized by the two high supersaturation methods, whereas the catalyst prepared at low supersaturation conditions and without ultrasonication, presented the lowest acidity (both in terms of concentration of acid sites and strength) and the lowest selectivity for ethylene formation. Regarding sample cHT2, its high dehydration activity may be related to its more noticeable acid character. The presence of a higher density of Al^{3+}–O^{2-} sites together with moderate-strength basic sites favours the formation of ethylene via E_2 elimination. This mechanism consists of a concerted-step requiring Lewis acid and basic sites of balanced strength so that no formation of ionic intermediates takes place [11]. Similar selectivity to ethylene was reached by sample cHT2US, in spite of exhibiting acid properties more similar to catalyst prepared at low supersaturation conditions than to cHT2. The explanation could be found in the considerably greater concentration of the strongest basic sites available in cHT2US catalyst, which would allow the dehydration to take place preferably through alternative E_{1cB} mechanism [11]. This pathway involves dissociative adsorption of an ethanol molecule on an acid-strong base pair site leading to an ethoxy intermediate. Then, a β-hydrogen in the ethoxy group is abstracted by a strong basic site forming a carbanion and, finally, the electron pair expels the oxygen and the double bond is formed.

Conversion of ethanol to acetaldehyde, taking into account outgoing acetaldehyde as well as condensed into heavier compounds, was especially important on c1HT catalyst and presented practically equal values of selectivity for the other three samples.

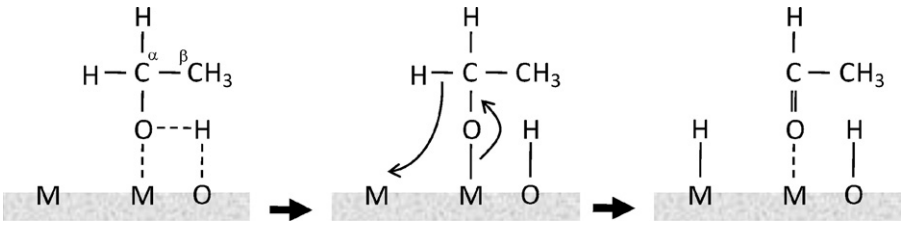

Scheme 2. Acetaldehyde formation mechanism in ethanol conversion reaction.

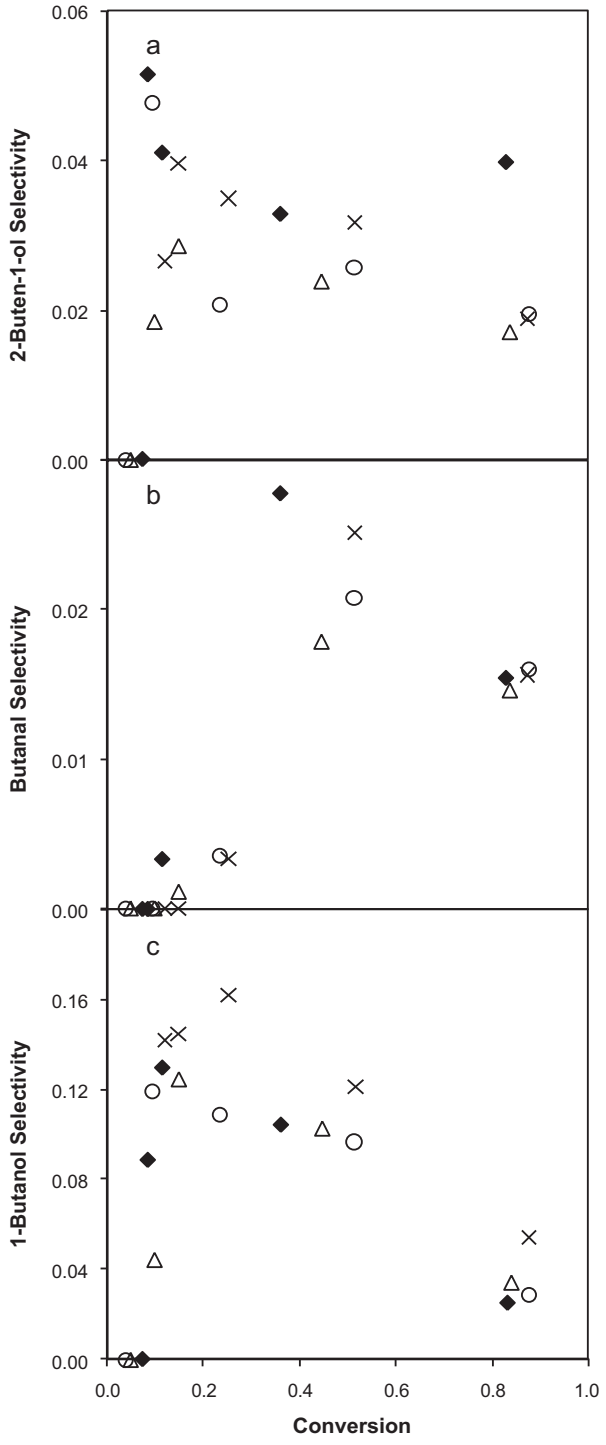

Fig. 4. Selectivity-conversion curves for partial o totally hydrogenated C4s: 2-buten-1-ol (a), butanal (b) and 1-butanol (c) over the tested catalysts: cHT1 (♦), cHT1US (○), cHT2 (△) and cHT2US (×).

Likewise, concentration of medium strength basic sites, corresponding to Mg^{2+}–O^{2-} pairs, in c1HT sample stands out from the remaining catalysts (see Table 2), which is consistent with the proposed reaction mechanism sketched in Scheme 2. In the first step, ethanol from gas phase is adsorbed on a Mg^{2+}–O^{2-} pair. Then, abstraction of the adsorbed hydrogen leads to a surface ethoxy intermediate that undergoes dissociation into aldehyde intermediate and hydride-like hydrogen involving a neighbouring acid site [10].

Concerning the condensation reactions, results must be discussed considering both the selectivity for the primary condensation product (2-butenal) and also the total selectivity for C4 products. Both selectivities are represented in Fig. 3a and b, respectively. In general trends, cHT1 material is the most selective at low conversions, probably because this material is the most selective for acetaldehyde formation, therefore being higher the surface concentrations of acetaldehyde in the surface. At higher conversion, this trend is reversed; being the catalysts prepared at high supersaturation conditions the most selective. For explaining this behaviour, it must be considered that the aldol condensation needs both the

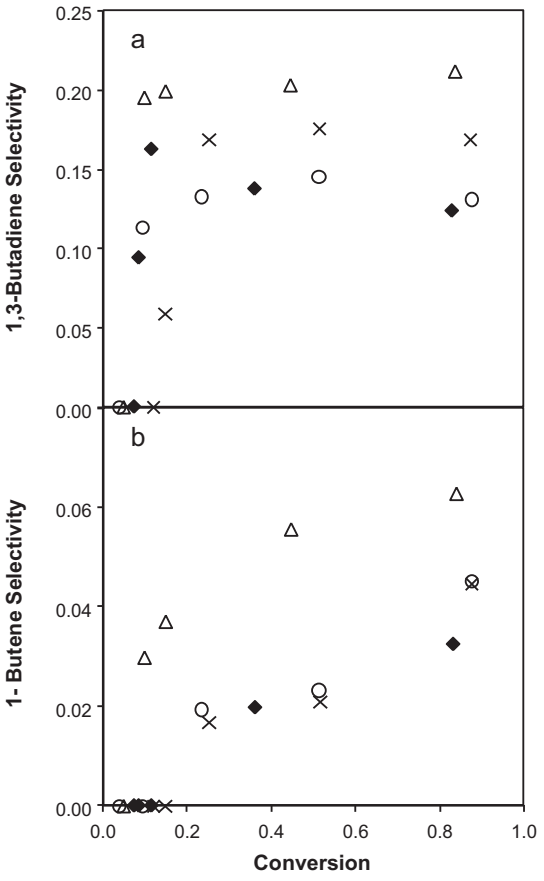

Fig. 5. Selectivity-conversion curves for C4 olefines: 1,3-butadiene (a) and 1-butene (b) over the tested catalysts: cHT1 (♦), cHT1US (○), cHT2 (△) and cHT2US (×).

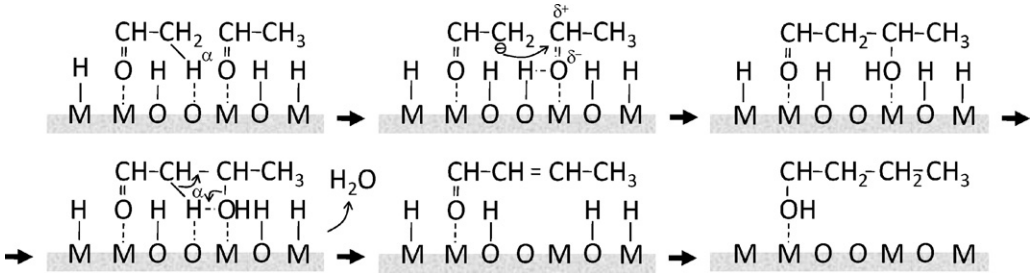

Scheme 3. Aldol condensation pathway from adsorbed acetaldehyde molecules.

presence of strong basic sites and acid–base pairs [11]. Therefore, as summarized in Scheme 3, reaction takes place between two adsorbed acetaldehyde molecules, starting with the abstraction of a α-hydrogen from one of the acetaldehyde molecules. However, the acidity of this α-H is lower than the acidity of the hydrogen from the ethanol hydroxyl group, needing stronger basic sites for getting this abstraction. The resulting carbanion (enolate) attacks the electrophilic carbon in the neighbouring acetaldehyde to form an aldol. A α,β-unsaturated aldehyde (2-butenal) is subsequently obtained by dehydration of the aldol.

Concerning the subsequent reactions of the 2-butenal, the hydrogenation of the C=O double bond (yielding 2-buten-1-ol, as observed in Fig. 4a) seems to be more favoured on the catalysts cHT1 and CHT2US, suggesting that the presence of weaker basic sites (such as the corresponding to bidentate and bicarbonate adsorption modes) can play a key role in this reactions. Similar behaviour is observed (Fig. 4b and c) for the formation of butanal and 1-butanol. Both products are often found as by-products in MPV reactions [32]. For the case of 1-butanol, it is remarkable the superior behaviour of the cHT2US materials, in good agreement with its more marked basic character.

Concerning to the formation of C4 olefins, butadiene is the predominant C4 olefin. In this case, the hydrotalcites prepared at high supersaturation conditions presented the highest selectivity, especially the prepared without sonication. As in the case of the formation of ethylene from ethanol discussed above, dehydration to 1,3-butadiene over the sample cHT2 seems to be mainly ascribed to the highest surface acidity of this material. Similar findings had been reported by Tsuchida et al. [10], who observed a correlation between the acidity of hydroxyapatite catalyst and the 1,3-butadiene yield.

In the light of the exposed results, the preparation that best fits the requirements of the ethanol catalytic condensation reaction, regarding C4 yield, is the high supersaturation method. Overall selectivity to C4 compounds was higher for cHT2 and cHT2US than for MgO catalysts tested at similar conditions [8], as well as for other Mg–Al mixed oxides reported in the literature [11]. Selectivity to 1-butanol did not reach values as high as those reported for an optimized formulation of a hydroxyapatite catalyst [3]. However, to the best of our knowledge, selectivity to butadiene on cHT2US and, especially, cHT2 catalyst was substantially better.

4. Conclusions

Although hydrotalcite-derived catalysts are promising catalysts for ethanol condensation reactions, the presence of acid sites promotes dehydration reaction, yielding ethylene. These side reactions are more important as reaction temperature increases.

The hydrotalcite preparation procedure affects its catalytic performance, being this effect caused by the observed variations on the concentration and distribution of acid and basic sites. The catalysts prepared at high supersaturation conditions present the best performance, which is mainly related with the presence of the strongest basic sites.

Acknowledgments

This work was supported by the Spanish Government (contract CTQ2008-06839-C03-02). M. León thanks the Government of the Principality of Asturias for a Ph.D. fellowship (Severo Ochoa Program).

References

[1] J. Franckaerts, G.F. Froment, Chem. Eng. Sci. 19 (1964) 807.
[2] A. Peloso, M. Moresi, C. Mustachi, B. Soracco, Can. J. Chem. Eng. 57 (1979) 159.
[3] T. Tsuchida, S. Sakuma, T. Takeguchi, W. Ueda, Ind. Eng. Chem. Res. 45 (2006) 8634.
[4] Y. Ono, T. Baba, Catal. Today 38 (1997) 321.
[5] K. Tanabe, W.F. Hölderich, Appl. Catal. A: Gen. 181 (1999) 399.
[6] W.F. Hoelderich, Catal. Today 62 (2000) 115.
[7] M.J. Climent, A. Corma, S. Iborra, A. Velty, J. Mol. Catal. A: Chem. 182–183 (2002) 327.
[8] A.S. Ndou, N. Plint, N.J. Coville, Appl. Catal. A: Gen. 251 (2003) 337.
[9] C. Carlini, C. Flego, M. Marchionna, M. Noviello, A.M. Raspolli Galletti, G. Sbrana, F. Basile, A. Vaccari, J. Mol. Catal. A: Chem. 220 (2004) 215.
[10] T. Tsuchida, J. Kuboa, T. Yoshioka, S. Sakuma, T. Takeguchi, W. Ueda, J. Catal. 259 (2008) 183.
[11] J.I. Di Cosimo, V.K. Díez, M. Xu, E. Iglesia, C.R. Apesteguía, J. Catal. 178 (1998) 499.
[12] M.J.L. Gines, E. Iglesia, J. Catal. 176 (1) (1998) 155.
[13] A.M. Hilmen, M. Xu, M.J.L. Gines, E. Iglesia, Appl. Catal. A: Gen. 169 (2) (1998) 355.
[14] J.I. Di Cosimo, C.R. Apesteguía, M.J.L. Ginés, E. Iglesia, J. Catal. 190 (2000) 261.
[15] R.E. Kirk, D.F. Othmer, Encyclopedia of Chemical Technology, vol. 4, fourth ed., John Wiley & Sons Inc., New York, 1997.
[16] K. Weissermel, H.J. Arpe, Industrial Organic Chemistry, Verlag Chemie, Berlin, 1978.
[17] F. Cavani, F. Trifirò, A. Vaccari, Catal. Today 11 (1991) 173.
[18] V.K. Díez, C.R. Apesteguía, J.I. Di Cosimo, J. Catal. 215 (2003) 220.
[19] S.K. Sharma, P.K. Kushwaha, V.K. Srivastava, S.B. Bhatt, R.V. Jasra, Ind. Eng. Chem. Res. 46 (2007) 4856.
[20] V.R.L. Constantino, T.J. Pinnavaia, Inorg. Chem. 34 (1995) 883.
[21] F. Prinetto, G. Ghiotti, R. Durand, D. Tichit, J. Phys. Chem. B 104 (2000) 11117.
[22] M.J. Climent, A. Corma, S. Iborra, K. Epping, A. Velty, J. Catal. 225 (2004) 316.
[23] X. Duan, D.G. Evans, Layered Double Hydroxides, Springer, Berlin, 2006.
[24] M. León, E. Díaz, S. Bennici, A. Vega, S. Ordóñez, A. Auroux, Ind. Eng. Chem. Res. 49 (2010) 3663.
[25] D. Carriazo, M. del Arco, C. Martín, V. Rives, Appl. Clay Sci. 37 (2007) 231.
[26] R. Jenkins, R.L. Snyder, Introduction to X-ray Powder Diffractometry, John Wiley & Sons Inc., New York, 1996.
[27] M. Ai, J. Catal. 40 (1975) 318.
[28] A. Gervasini, A. Auroux, J. Catal. 131 (1991) 190.
[29] M.A. Aramendía, V. Borau, C. Jiménez, J.M. Marinas, A. Porras, F.J. Urbano, J. Catal. 161 (1996) 829.
[30] V.K. Díez, C.R. Apesteguía, J.I. Di Cosimo, Catal. Today. 63 (2000) 53.
[31] J.I. Di Cosimo, A. Acosta, C.R. Apesteguía, J. Mol. Catal. A: Chem. 222 (2004) 87.
[32] F.J. Urbano, M.A. Aramendía, A. Marinas, J.M. Marinas, J. Catal. 268 (2009) 79.